Characterization of New Surface Morphologies
in a Hydrogen-Bonded Multilayer System

by

Allison Kunz

Submitted to the Department of Materials
Science and Engineering in Partial
Fulfillment of the Requirements
for the Degree of

Bachelor of Science

at the

Massachusetts Institute of Technology

December 2007
[June 2008]

Signature of Author .....
Department of Materials Science and Engineering
December 11, 2007

Certified by .....
Michael F. Rubner
TDK Professor of Materials Science and Engineering
Thesis Supervisor

Accepted by .....
Caroline A. Ross
Chairman, Undergraduate Thesis Committee

Characterization of New Surface Morphologies in a Hydrogen-Bonded Multilayer System

This work presents an analysis of surface morphology changes in poly(acrylic acid)/polyacrylamide (PAA/PAAm) hydrogen-bonded multilayers. These changes were induced by immersion of the films in aqueous solutions of poly(allylamine hydrochloride), or PAH, at different levels of pH. Positive charges on PAH are attracted to negative charges on PAA, forming ionic bonds and locally decreasing the hydrophilicity of the multilayer. The degree of ionization for each polyelectrolyte, controlled by the pH of the treatment solution, determines the molecular conformations and the extent of electrostatic interactions. These factors, in turn, determine the resulting morphology of the film. Different surface morphologies appeared in four different pH regimes. Highly acidic solutions retained the film's original smooth surface, but wrinkled, honeycomb, or globular morphologies appeared as the pH increased. The three different surface morphologies correlate with the linear, pearl necklace, and globular conformations of PAH.

A popular method of surface modification is through the use of polyelectrolyte multilayers. By careful selection of the specific polymers used, the properties of the final film can be tailored for a vast range of applications. For example, previous literature has reported simple multilayers that resist cell adhesion[1]: multilayer coatings could cheaply and easily prevent infection or rejection of biomedical devices. Utilization of the polymers' functional groups provide further possibilities: antibacterial films through nanoreactor chemistry[2], selective cell adhesion or repulsion through the chemical adhesion of peptides[3], and multilayer-coated membranes that swell or contract according to the pH of the passing fluid[4]. Innovative patterning techniques such as photolithography[5] and stamping[6] add even more options. Indeed, a nearly infinite number of combinations of different polymers and processes exist for making uniquely useful polymer surfaces.

The underlying concept is simple: by immersing a substrate in alternating baths of polycationic and polyanionic solutions, electrostatic attraction results in the building of polymer

films. This manufacturing concept, known as layer-by-layer deposition (LbL), utilizes easily programmable "dipping machines" which can process batches of samples at a time. Industrial uses of multilayer thin films have also implemented spraying methods to accommodate continuous large-scale production. After deposition, the film is usually crosslinked to provide stability in a range of environments. Thermal, chemical, or UV crosslinking forges covalent bonds between the polymers by using heat, chemistry, or ultraviolet light, respectively.

Alternatively, polymers can be selectively dissolved out of the multilayer to create porous films[7] or their conformations altered with salt[8] solutions to create rough films. Rubner et al created microporous films by immersion of a polyelectrolyte multilayer in an acid bath.[9] Later work found that a system of two acid baths created a much rougher surface, which was then used as a base for superhydrophobic films.[10] Further research characterized the acid-induced nanoporosity and microporosity of this multilayer, with and without combination with another multilayer system, and then successfully used these pores as drug delivery mechanisms.[11] Surface roughness or porosity can provide useful and tunable surface properties.

This research studies the hydrogen-bonded multilayer made with poly(acrylic acid), abbreviated as PAA, and polyacrylamide, or PAAm. This system is not a true polyelectrolyte multilayer, utilizing hydrogen rather than ionic bonds, but the term "polyelectrolyte thin film" is often extended to this system. PAAm is a neutral polymer with an amide functional group. PAA, a weak polyelectrolyte with a carboxylic acid group, can participate in either hydrogen or ionic bonding depending on the pH of the solution. Thermal crosslinking creates strong imide bonds between the two polymers in a condensation reaction with water as a byproduct. PAA/PAAm multilayers are commonly used in biotechnology research including the previously mentioned antibacterial and selective cell adhesion applications. This system has been extensively

characterized, and the present work consists of a curious phase change found (unintentionally) during an experiment that has since been published. More recently this phenomenon has been reported in the work by Van Vliet et al, which studied the mechanical properties of PAA/PAAm films[12]. They observed that the adsorption of poly(allylamine hydrochloride), or PAH, in solution resulted in a phase change and an increase of the modulus of the original film by over two orders of magnitude. Interestingly, stamping of PAH on to the surface also increased the modulus, but to a much smaller extent. A full theory behind these observations was not given:

> ...it is possible that this adsorption step induced potential phase transitions/separations, which would be consistent with the observed slight change in opacity of the PEM upon PAH adsorption, and this possible phase transition is currently under investigation.

After deposition and thermal crosslinking, immersion of this initially flat film in a solution of PAH results in fascinating new surface morphologies. Our observations correlate closely with those of Van Vliet et al, and we provide a characterization and thorough explanation of this phenomenon. The purpose of this paper is to outline a theory of how and why this phenomenon occurs.

Experimental Section

Materials. Poly(acrylic acid) (MW 90,000; 25 wt % solution), polyacrylamide (MW 800,000; 10 wt % solution), linear polyethylenimine (PEI; MW 25,000), and poly(vinylamine hydrochloride) (PVAm; MW 25,000) were obtained from Polysciences. Poly(allylamine hydrochloride) (MW 70,000 and MW 15,000) was obtained from Sigma Aldrich in both standard and FITC-labeled forms. The structures of PAA and PAAm are illustrated in Scheme 1. Silane-prep (aminoalkylsilane) glass slides were also obtained from Sigma Aldrich. Deionized filtered water came from a Millipore Milli-Q system, with a pH of approximately 5.6.

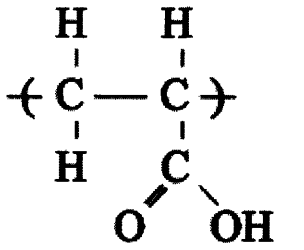

a) Poly(acrylic acid)

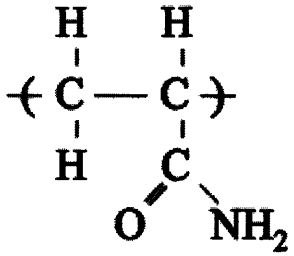

b) Polyacrylamide

Scheme 1. Structures of a) PAA and b) PAAm

Sample Preparation. All samples were prepared by LbL deposition with an automated dipping machine (Zeiss HMS series Programmable Slide Stainer). Each bilayer was deposited by immersion of a silane-prep glass slide into a 20 mM solution of PAA, followed by three deionized water (DIW) rinse baths of 2, 2, and 1 minutes each, and then a reiteration of these steps for PAAm. Both the polymer solutions and rinse baths were pH adjusted to 3.0. After deposition of 10.5 bilayers, the samples were thermally crosslinked at 100°C for 24 hours.

All experiments consisted of immersion of samples in a treatment solution for 15 minutes, followed by two DIW rinse baths for 5 and 2 minutes each. The rinse baths were pH-adjusted to match the pH of the treatment solution. The treatment solutions varied by experiment, but all polymer solutions had a concentration of 20 mM.

Sample Analysis. Images of all sample surfaces were taken using an atomic force microscope (AFM, Digital Instruments D3100) in tapping mode. The AFM's software (v5.31r1) was used to find root mean square (RMS) roughness data from each image, providing a useful measure of the degree of change. (Roughness data should be considered accurate to within +/- 3 nm.) All AFM images shown in this paper are 15 μm by 7.5 μm, with a z scale of 250 nm, unless noted otherwise. Thickness measurements utilized a simple scratch test: the glass slides were scored with the tip of a steel razor blade, and a profilometer (Tencor P-10 surface profiler) measured the resulting step height.

Solute Effects. Samples were immersed in treatment solutions with a range of solutes: DIW with 10mM NaCl, unmodified PAH (pH 3.8), and PAH with 10mM NaCl (pH 4.2). Untreated samples and samples treated with pure DIW (pH 5.6) were included as controls.

pH Effects. The effect of pH on the surface morphology was found through a series of PAH treatments over a range of pH: 1.5, 3.0, 7.0, 8.6, and 11.3.

MW Effects. Treatments of PAH with different molecular weights (70,000 or 15,000) were given at both pH 3.8 (unadjusted) and pH 8.6 in order for direct comparison of multiple types of surface morphologies.

Time Study. Samples were immersed in PAH treatment solutions of pH 8.6 for 5 seconds, 30 seconds, 15 minutes, 30 minutes, 3 hours, 8 hours, 17 hours, and 98 hours in order to observe any changes in surface morphology over time.

Temperature Study. This experiment also probes the kinetics of the phase change by depositing PAH at an elevated temperature of 44°C and a lowered temperature of 3°C. Heating and cooling were accomplished using a hot plate and an ice bath, respectively, and the temperature was monitored using a thermocouple.

Reversability. Samples that had been previously treated with PAH at pH 8.6 were immersed in DIW with the much lower pH values of 3.0 and 1.5 in an attempt to regain the films' initially smooth state.

Fluorescence. Treatments of FITC-labeled PAH were given over a range of pH: 1.5, 4.2, and 11.3. A 100.5 bilayer sample was treated with pH 8.6 PAH and examined using both confocal and fluorescence microscopy. Profilometry of this sample measured a post-treatment film thickness of approximately 10 microns.

Treatment Polycation Amine Group. This experiment varies the number of methyl groups between the amine and the polymer backbone of the absorbing polyelectrolyte. Instead of PAH, treatment solutions contained pH 8.6 linear PEI or PVAm.

Results

These experiments were designed to pinpoint under which conditions the new surface morphologies occurred, and to gain insight into the molecular mechanisms behind the macroscopic changes.

The solute experiments confirmed the role of PAH in the creation of these new surface morphologies. Multilayers treated with DIW, either unmodified or with salt, were as smooth as the original films. The addition of PAH resulted in a rougher, well-defined texture. Salt seems to aid in the texturing process, as seen by the large increase in roughness compared to PAH alone, but it does not invoke any morphological changes on its own. The dissolved salt most likely shifts the effective pKa of PAA and PAH, resulting in the emergence of the honeycomb structure at a lower pH. Figure 1 provides AFM images and RMS roughness values for each treatment.

PAH has now been identified as the key factor, but the behaviors of multilayer films and polyelectrolytes often rely on pH. In Figure 2, we see that different pH regimes result in varying surface morphologies. At the extremely low pH of 1.5, no changes are seen between treated and untreated films. At pH 3.0 (and pH 4.2 from Figure 1), a wrinkled texture appears on the surface and the RMS roughness increases slightly. At pH 7.0 and 8.6, the surface morphology becomes a very rough and dramatic honeycomb texture. For pH 11.3, the film has a relatively flat, globular appearance with lower roughness.

Molecular weight of PAH had no significant effect on the surface morphology. The AFM images in Figure 3 for pH 3.8 and 8.6, with wrinkled and honeycomb morphologies, respectively, are nearly identical for both high (70,000) and low (15,000) molecular weights.

The kinetics of morphological change was studied by varying treatment time and temperature. Figure 4 shows AFM images of samples that were left in pH 8.6 PAH solution for times ranging from 5 seconds to 98 hours. The morphological change from smooth to honeycomb-like begins within 5 seconds of immersion and reaches maximum roughness within 15 minutes. The honeycomb structure remains stable for several hours. After a long period in solution, over four days, the honeycomb ridges have begun to subside. The thickness of the film had not decreased according to profilometry, indicating that the film itself had not dissolved into solution. It is more likely that the molecules in the multilayer had slowly shifted in order to lower the stresses around the steep honeycomb walls. Temperature also had little effect on the honeycomb structure. Lowering the temperature of the pH 8.6 PAH treatment solution to 3°C slowed the down the morphological change enough so that it had not quite reached maximum roughness by the end of 15 minutes (Figure 5). However, increasing the temperature does not increase the maximum roughness.

therefore no PAH adsorbs onto the surface of the film. No orange color is observed on the FITC-PAH samples, and no changes to the film are evident in the AFM images.

The moderately acidic treatment solutions, from pH 3.0 to 4.4, create a fraction of negatively charged carboxylic acid groups on PAA. These negative charges now attract the positively charged amines from PAH. PAH, which is in its linear conformation, adsorbs onto the surface of the film and creates the interesting texture seen in the AFM images. The very faint color of the FITC-labeled samples indicates that not much PAH is adsorbing onto the film surface, which in turn strongly suggests that the fraction of charged functional groups on PAA is very small: the system has not yet reached its pKa. This finding differs from the reported fall in pKa of PAA to less than 3.0 in ionic-bonding multilayers such as PAA/PAH. Evidently, the hydrogen bonds do not enhance the weak polyanion's ability to deprotonate in the same manner as a positively charged environment. Also, the degree of ionization is such that the majority of hydrogen bonds still remaining between PAA and PAAm prevent PAH from diffusing into the film.

At higher pH, specifically 7.0 and 8.6, a growing majority of the carboxylic acid groups of PAA become negatively charged and the pearl necklace structure of PAH emerges as its degree of ionization begins to fall. The high degree of ionization of PAA causes the multilayer to swell; adjacent negative charges along the molecules repel each other, causing these polymers to extend themselves as much as possible within the limitations imposed by crosslinks. The PAH is able to diffuse into the swollen film as well as adhere to the surface, as evidenced by the confocal microscopy. The increased stiffness reported by Van Vliet et al can be attributed to the PAH inside the multilayer. The opposite charges of PAH and PAA create ionic crosslinking which stiffens the film. Logically, some form of phase separation occurs due to PAH changing

the local multilayer composition. The fluorescence image shows that the honeycomb ridges contain high concentrations of PAH, indicating that the pearl necklace molecules on the film surface tend to associate into hydrophobic structures. The regions of ionic crosslinking in the multilayer have also become effectively more hydrophobic. These hydrophobic associations cause a phase separation between the originally hydrophilic multilayer and the new hydrophobic regions with incorporated PAH. The covalent crosslinks constrain the distance of separation, resulting in the honeycomb morphology rather than the usual random globules associated with spinodal decomposition. The crosslinking constraints also explain why temperature did not affect the size of the honeycomb "pores:" the degree of covalent crosslinking and therefore the possible distance of separation was held constant for those samples. The hydrophobic nature of the deprotonated amine definitely correlates with the ability of the adsorbing polyelectrolyte to form these ridged structures: the experiments with PEI and PVAm show a decrease in roughness with smaller hydrophobic side groups.

High pH results in a very high degree of ionization for PAA and a low degree of ionization for PAH. The multilayer presents a large, negative surface that strongly attracts all available positive segments of PAH, and each positive segment carries a large globular structure with it. A large amount of PAH becomes attached to the film surface, as shown by the distinctly orange hue of the film. Unlike the previous pH regime, when PAH in its pearl necklace conformation diffused into the swollen multilayer, diffusion into the film is unlikely due to the large size of the PAH globules. Visualizations of these different interaction regimes are provided in Figure 10.

Immersion of samples with the honeycomb structures into DIW with low pH did not succeed in reversing the morphological change. As shown in Figure 6, treatment of pH 3.0 DIW actually increased the roughness slightly. Neither the height of the honeycomb walls nor the average distance between them changed perceptibly. Treatment of pH 1.5 DIW managed to flatten the film considerably, but the roughness was still greater than the initially smooth multilayer and the honeycomb texture was still clearly evident.

FITC-labeled PAH, which has a bright orange color, confirmed the level of adsorption at the different pH regimes. Visual inspection observed that treatment at pH 1.5 left no orange color, pH 4.4 showed faint color, and pH 11.3 resulted in distinctly orange films. AFM images, not shown, confirmed that these treatments resulted in the same types of surface morphologies as their non-fluorescent counterparts. Confocal microscopy of a 10-micron thick (100.5 bilayer) film indicated that PAH had diffused into the entirety of the film and concentrated in the honeycomb ridges. The fluorescence microscope image given in Figure 7 shows the concentration of PAH in the honeycomb ridges.

Adsorbing polycations with slightly different chemical structures resulted in very different surface morphologies even at the same pH of 8.6. The amine groups of PVAm are connected directly to the main chain, and linear PEI has the amine incorporated into the backbone. These are structurally similar to the functional amines of PAH, which are connected to the main chain by two methyl groups. As illustrated in Figure 8, PEI resulted in a wrinked structure similar to that of PAH between pH 3.0 and 4.2, while PVAm resulted in the creation of many small pores.

Discussion

The data indicates that treatment of a $(PAA/PAAm)_{10.5}$ multilayer film with PAH will yield one of four different surface morphologies, depending on the pH of the treatment solution: flat, slightly wrinkled, honeycomb, and globular. pH controls the degree of ionization of the polyelectrolytes, and therefore it dictates their conformation and interactions. By taking into account the degree of ionization and consequent intermolecular forces between each of the constituent polymers, we can build a coherent theory about the morphology mechanisms.

The PAA/PAAm system remains stable even at high pH due to the covalent crosslinks. Previous literature by Rubner et al specifically documented this stability at high pH and long times by FT-IR. Therefore, this multilayer's change in surface morphology relies on the addition of a polymer rather than the methods of selective removal used by other recent works in order to obtain a rough or porous surface referred to previously.

Although the film remains intact, varying pH does cause significant changes in the multilayer. The free carboxylic acid groups of PAA have a pKa of approximately 6.5 in solution and roughly less than 3.0[13] in a multilayer. Well below the value of 6.5 given for solutions, in this case pH 1.5, all of the carboxylic acid groups are protonated and neutral. Above this value, the majority of these groups become negatively charged, and by pH 11.3, PAA is fully ionized. PAAm remains charge neutral over the entire range of pH. PAH is deposited in solution, where the reported pKa is 8.8[14] for its amine group, but diffusion into a multilayer raises the pKa to over 10.0[15]. PAH and similar polycations undergo conformational changes at different degrees of ionization. Well below the pKa, all of the amine groups are protonated and carry a positive charge. The electrostatic repulsion caused by like charges result in an extended molecule where the amines stay as far apart as possible. When PAH is only partially ionized at higher pH values,

the charged amines continue to repel each other while the neutral amines begin to agglomerate into hydrophobic beads along the polymer chain. The size of the hydrophobic beads in this "pearl necklace" structure varies inversely with the degree of ionization[16,17]. At a high enough pH, the degree of ionization falls below a critical point and PAH collapses into a globular conformation. The pH-dependent behavior of PAA and PAH, summarized in Figure 9, is key to understanding the pH-dependent surface morphologies.

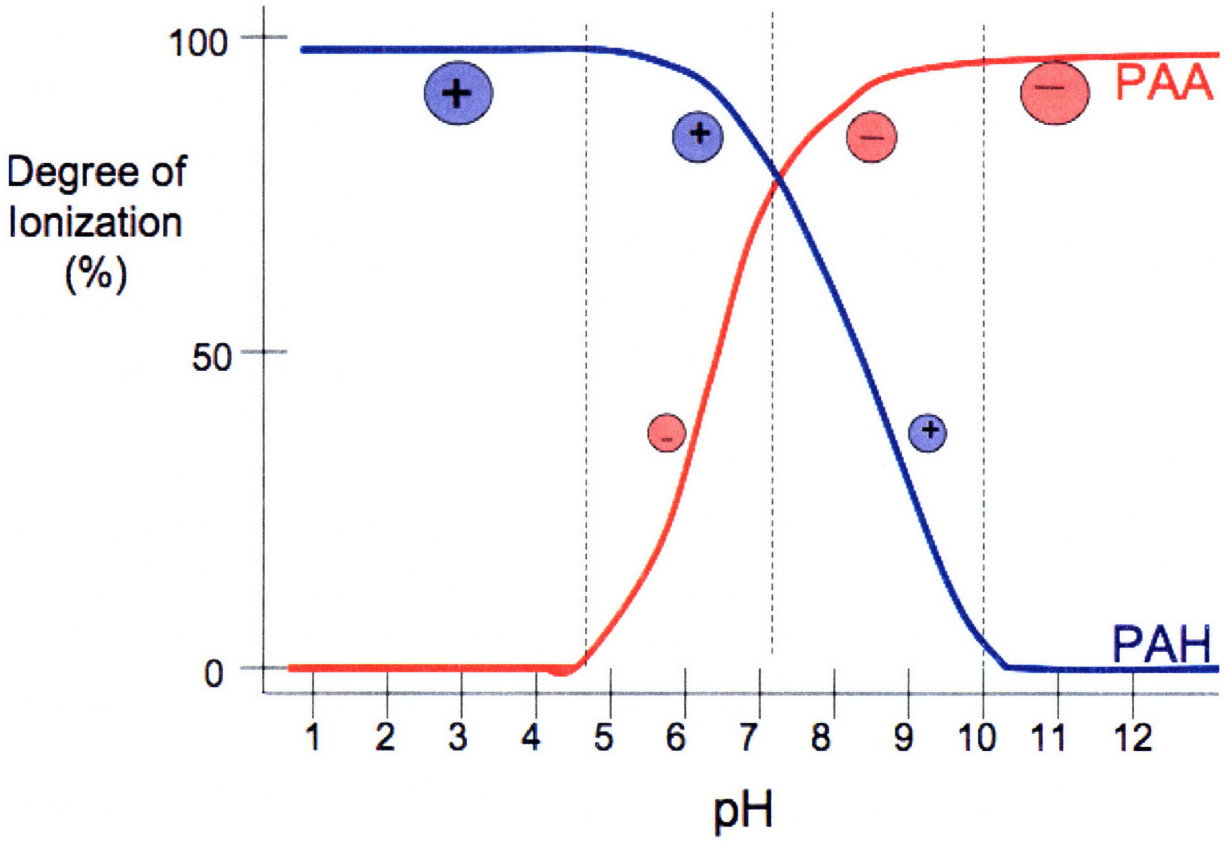

Figure 9. Degree of ionization of PAA and PAH in different pH regions.

In an extremely acidic environment, pH 1.5 for our experiments, the free (i.e., not crosslinked) neutral, protonated carboxylic acids from PAA form hydrogen bonds with the amide groups from PAAm. No electrostatic forces exist to attract the positively charged PAH, and

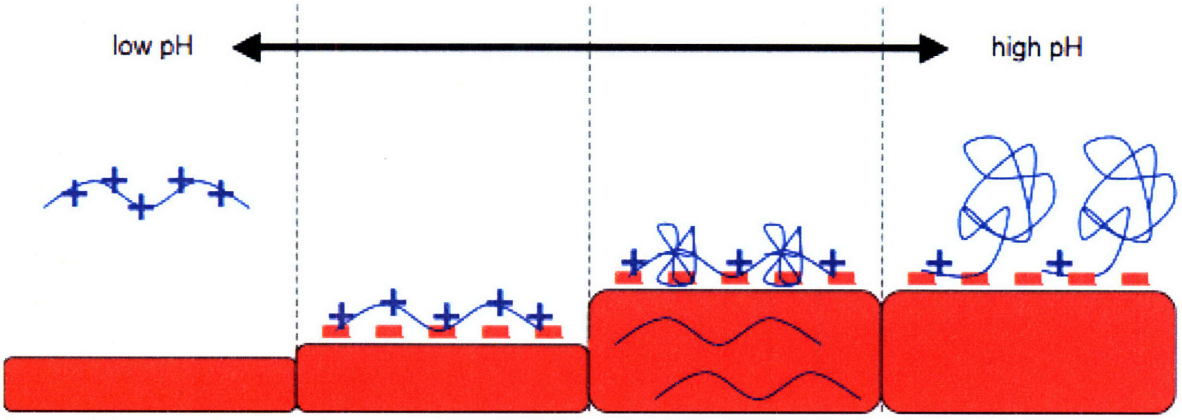

Figure 10. Schematic diagram of polymer interactions at different pH regimes. Red represents the multilayer, and blue represents PAH.

Future work would run additional experiments to confirm or modify the theory presented above and then focus on possible applications for these new rough surfaces. Additional fluorescence microscopy would confirm the extent diffusion of PAH into the multilayer at the different pH regions and the validity of the theory. Additional experiments with PEI and PVAm at other pH ranges would also provide useful corroborating information, especially with existing literature on PVAm "pearl necklace" and globular conformations by Borkovec et al.[17] A valuable contribution to the existing literature on hydrogen-bonded multilayers would be to make FT-IR samples over a range of pH to pinpoint the exact pKa of PAA in this type of system.

The most likely applications of this phenomenon would be related to biotechnology. *In situ* modulus values, which positively correlate with cell adhesion, would probably be different for each type of morphology. The honeycomb pattern should be evaluated as a potential tissue engineering scaffold. It would also be interesting to find out how bacteria react to this rough surface.

Acknowledgements

I would like to thank Jenny Lichter for her generous help in preparing this report. Daeyeon Lee provided the confocal microscope data and fluorescence images. David Bono provided the equipment (thermocouple device and power supply) for the temperature study.

---

[1] Yang, S. Y.; Mendelsohn, J. D.; Rubner, M. F. New class of ultrathin, highly cell-adhesion-resistant polyelectrolyte multilayers with micropatterning capabilities. *Biomacromolecules* **2003**, 4, (4), 987-994.
[2] Lee, D.; Cohen, R. E.; Rubner, M. F. Antibacterial properties of Ag nanoparticle loaded multilayers and formation of magnetically directed antibacterial microparticles. *Langmuir* **2005**, 21, (21), 9651-9659.
[3] Mendelsohn, J. D.; Yang, S. Y.; Hiller, J.; Hochbaum, A. I.; Rubner, M. F. Rational design of cytophilic and cytophobic polyelectrolyte multilayer thin films. *Biomacromolecules* **2003**, 4, (1), 96-106.
[4] Lee, D.; Nolte, A. J.; Kunz, A. L.; Rubner, M. F.; Cohen, R. E. pH-Induced hysteretic gating of track-etched polycarbonate membranes: swelling/deswelling behavior of polyelectrolyte multilayers in confined geometry. *J. Am. Chem. Soc.* **2006**, 128, (26), 8521-8529.
[5] Yang, S. Y.; Rubner, M. F. Micropatterning of polymer thin films with pH-sensitive and cross-linkable hydrogen-bonded polyelectrolyte multilayers. *J. Am. Chem. Soc.* **2002**, 124, (10), 2100-2101.
[6] Berg, M. C.; Yang, S. Y.; Hammond, P. T.; Rubner, M. F. Controlling mammalian cell interactions on patterned polyelectrolyte multilayer surfaces. Langmuir **2004**, 20, (4), 1362-1368.
[7] Fu, Y.; Bai, S.; Cui, S.; Qiu, D.; Wang, Z.; Zhang, X. Hydrogen-bonding-directed layer-by-layer multilayer assembly: reconformation yielding microporous films. *Macromolecules* **2002**, 35, (25), 9451-9458.
[8] Fery, A.; Scholer, B.; Cassagneau, T.; Caruso, F. Nanoporous thin films formed by salt-induced structural changes in multilayers of poly(acrylic acid) and poly(allylamine). *Langmuir* **2001**, 17, (13), 3779-3783.
[9] Mendelsohn, J. D.; Barrett, C. J.; Chan, V. V.; Pal, A. J.; Mayes, A. M.; Rubner, M. F. Fabrication of microporous thin films from polyelectrolyte multilayers. *Langmuir* **2000**, 16, (11), 5017-5023.
[10] Zhai, L.; Cebeci, F. C.; Cohen, R. E.; Rubner, M. F. Stable superhydrophobic coatings from polyelectrolyte multilayers. Nano Lett. **2004**, 4, (7), 1349-1353.
[11] Berg, M. C.; Zhai, L.; Cohen, R. E.; Rubner, M. F. Controlled drug release from porous polyelectrolyte multilayers. *Biomacromolecules* **2006**, 7, (1), 357-364.
[12] Thompson, M. T.; Berg, M. C.; Tobias, I. S.; Lichter, J. A.; Rubner, M. F.; Van Vliet, K. J. Biochemical functionalization of polymeric cell substrata can alter mechanical compliance. *Biomacromolecules* **2006**, 7, (6), 1990-1995.
[13] Shiratori, S. S.; Rubner, M. F. pH- dependent thickness behavior of sequentially adsorbed layers of weak polyelectrolytes. *Macromolecules* **2000**, 33, (11), 4213-4219.
[14] Choi, J.; Rubner, M. F. Influence of the degree of ionization on weak polyelectrolyte multilayer assembly. *Macromolecules* **2005**, 38, (1), 116-124.
[15] Itano, K.; Choi, J.; Rubner, M. F. Mechanism of the pH-induced discontinuous swelling/deswelling transitions of poly(allylamine hydrochloride)-containing polyelectrolyte multilayer films. *Macromolecules* **2005**, 38, (8), 3450-3460.
[16] Gopinadhan, M.; Ahrens, H.; Gunther, J.; Steitz, R.; Helm, C. A. Approaching the precipitation temperature of the deposition solution and the effects on the internal order of polyelectrolyte multilayers. *Macromolecules* **2005**, 38, (12), 5228-5235.
[17] Kirwan, L. J.; Papstavrou, G.; Borkovec, M. Imaging the coil-to-globule conformational transition of a weak polyelectrolyte by tuning the polyelectrolyte charge density. *Nano Lett.* **2004**, 4, (1), 149-152.

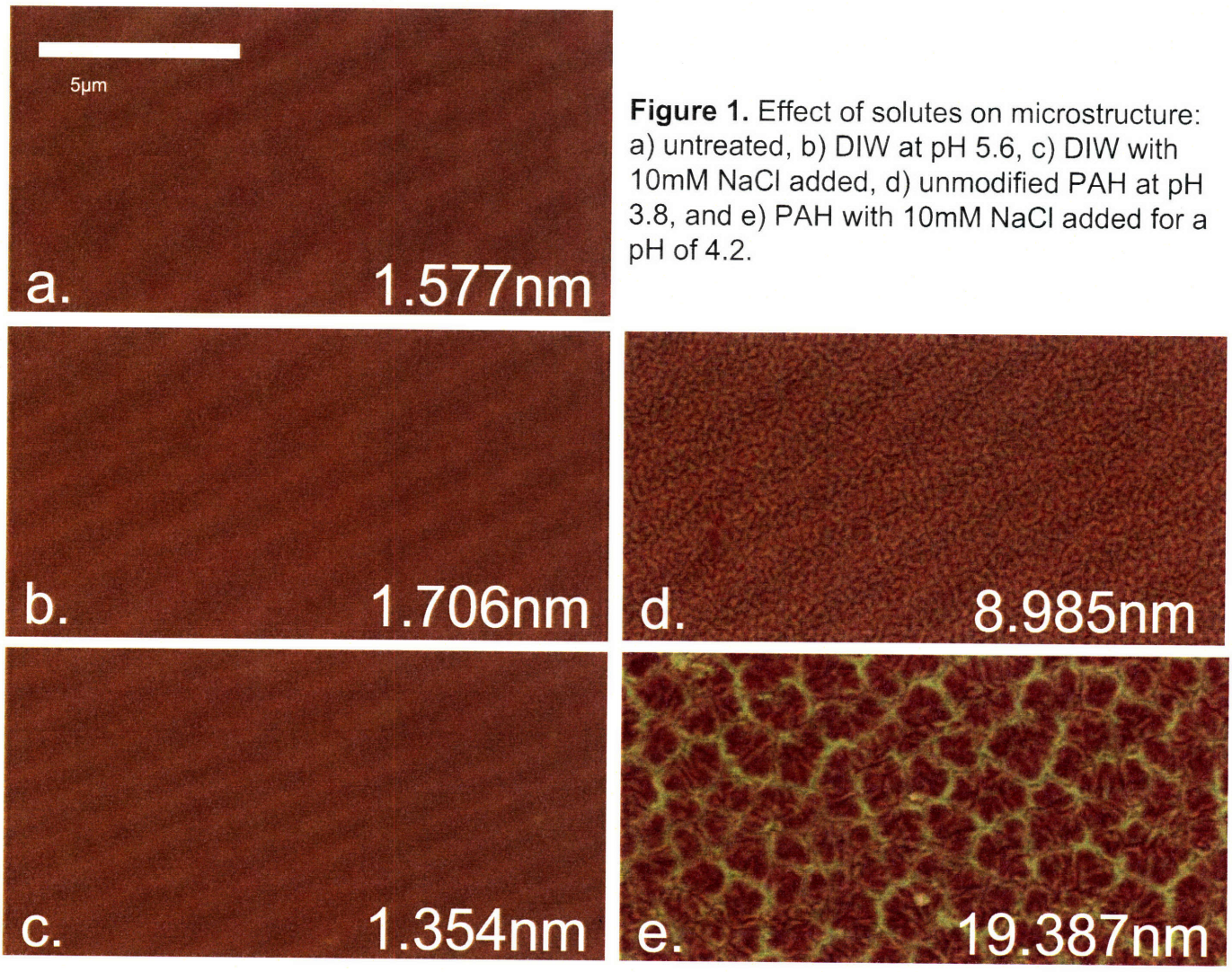

Figure 1. Effect of solutes on microstructure: a) untreated, b) DIW at pH 5.6, c) DIW with 10mM NaCl added, d) unmodified PAH at pH 3.8, and e) PAH with 10mM NaCl added for a pH of 4.2.

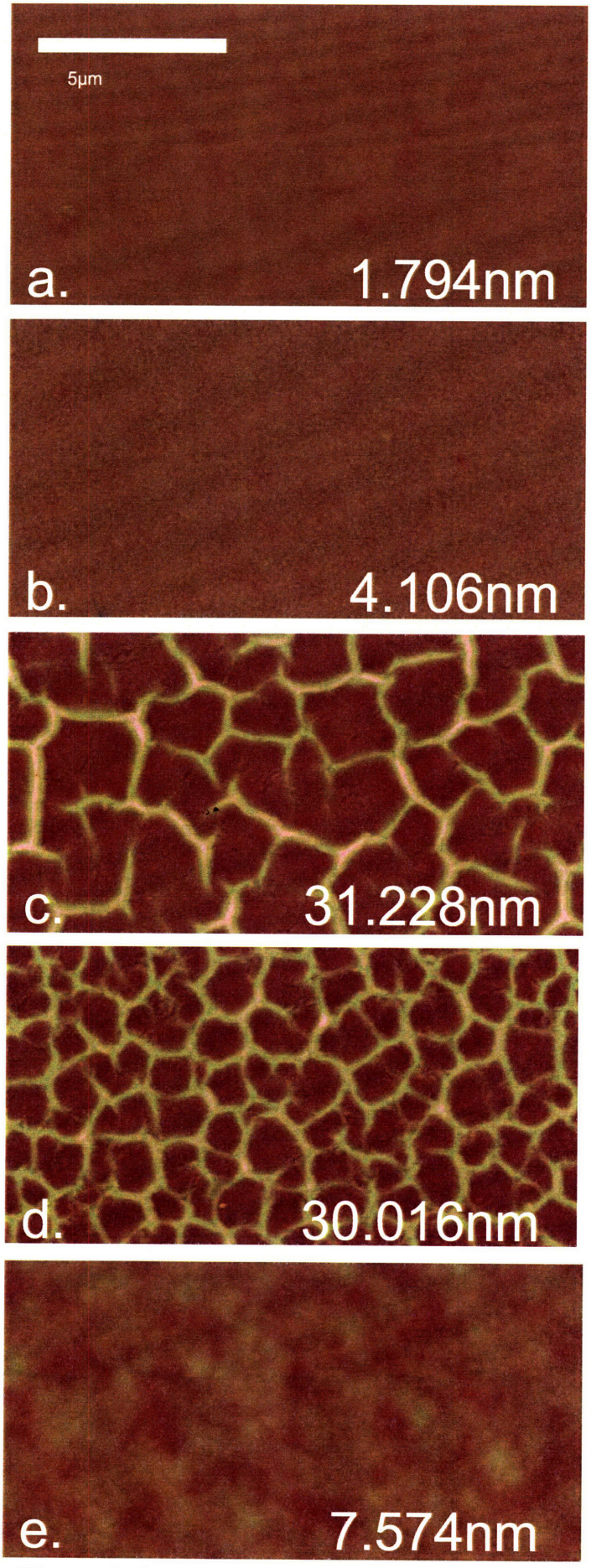

Figure 2. PAH treatment over a range of pH: a) 1.5, b) 3.0, c) 7.0, d) 8.6, and e) 11.3.

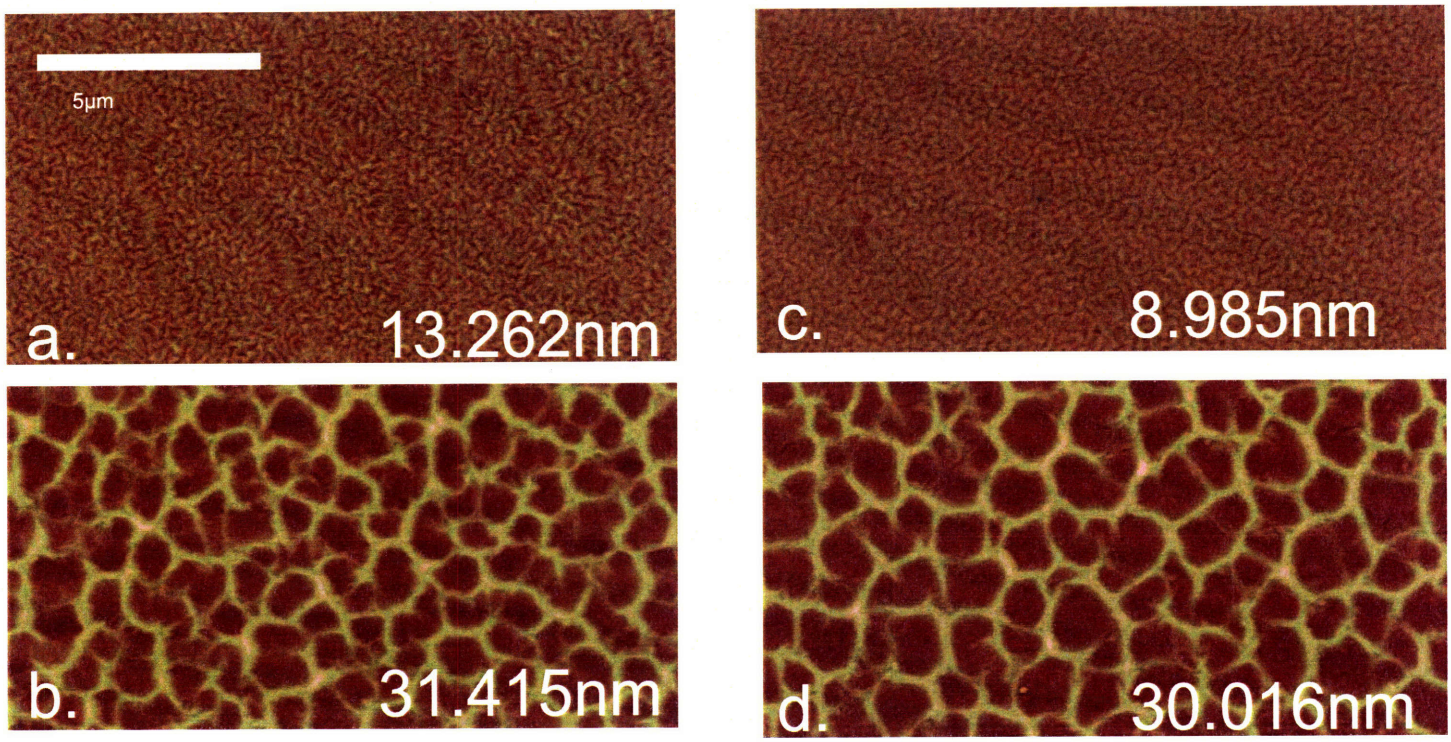

Figure 3. Effect of MW on microstructure: PAH 15k at a) natural pH of 3.8 and b) pH adjusted to 8.6, and PAH 70k at c) natural pH of 3.8 and d) pH adjusted to 8.6.

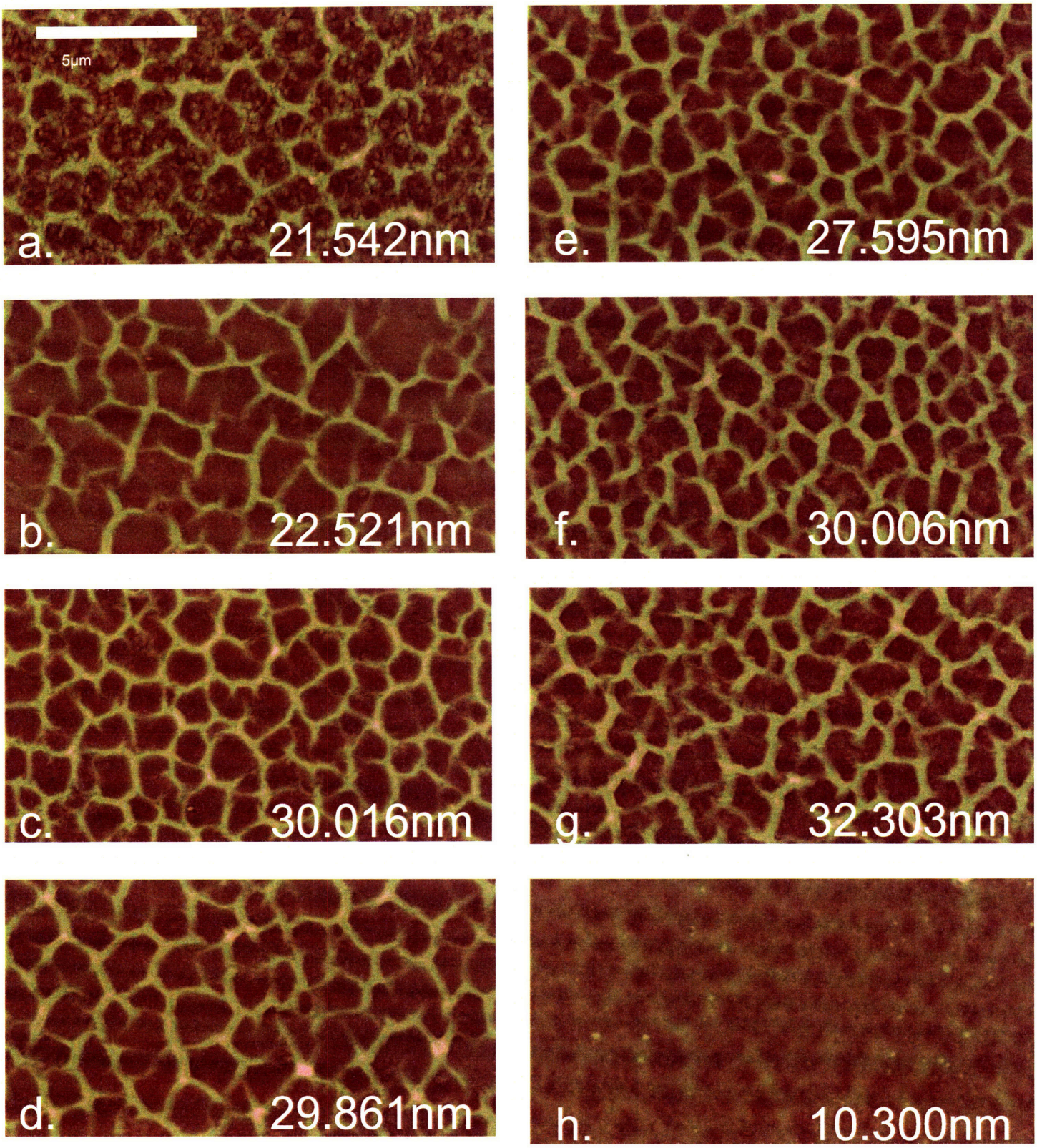

Figure 4. Time series data: these samples were left in pH 8.6 PAH solution for a) 5 seconds, b) 30 seconds, c) 15 minutes, d) 30 minutes, e) 3 hours, f) 8 hours, g) 17 hours, and h) 98 hours.

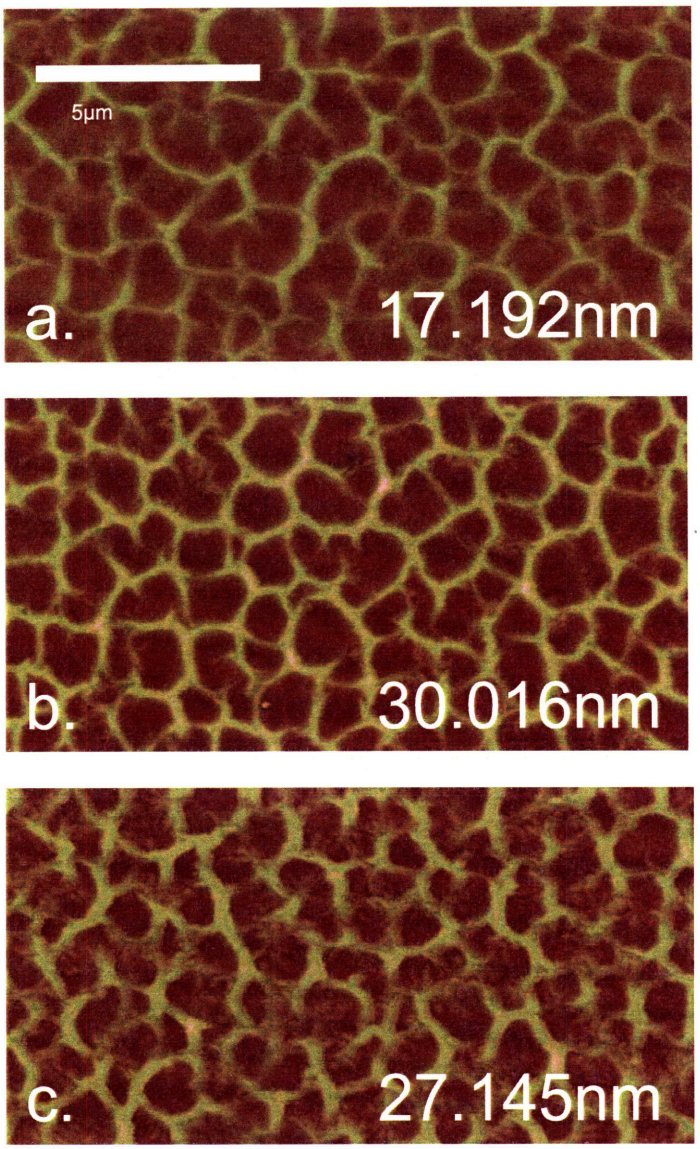

Figure 5. Temperature series data: these samples were treated in pH 8.6 PAH solutions at a) 3±2°C, b) 20±2°C, and c) 44±2°C.

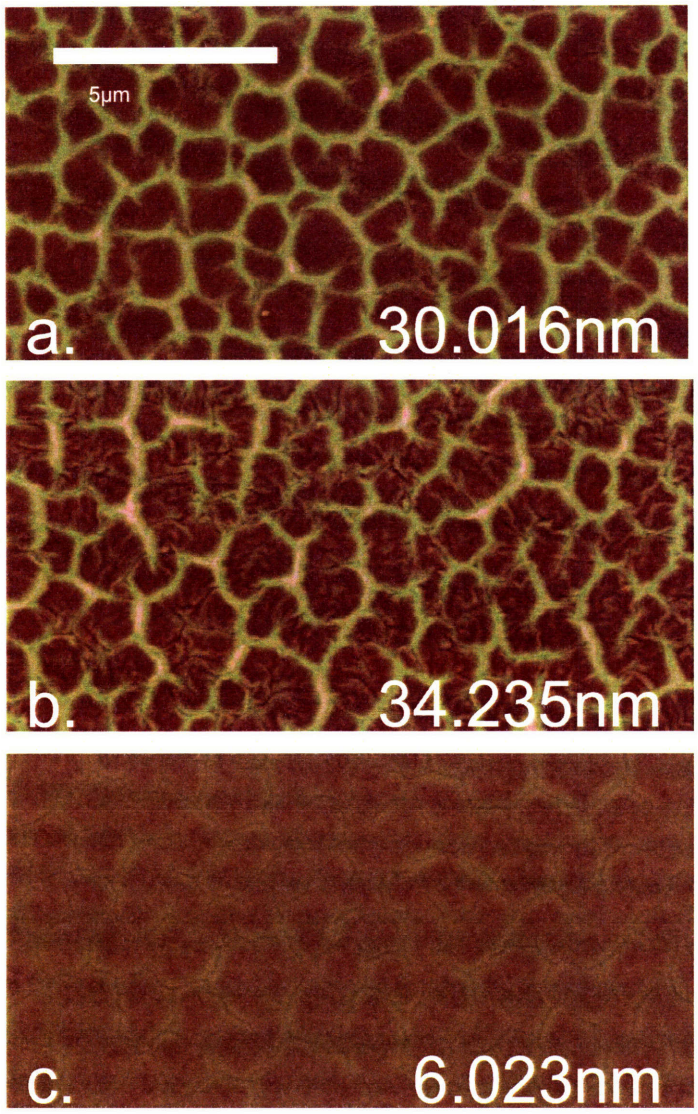

Figure 6. Attempts to reverse the changes in surface morphology from the the honeycomb found in a) to the original flat surface by immersion in b) DIW at pH 3.0 and c) DIW at pH 1.5 for 15 minutes.

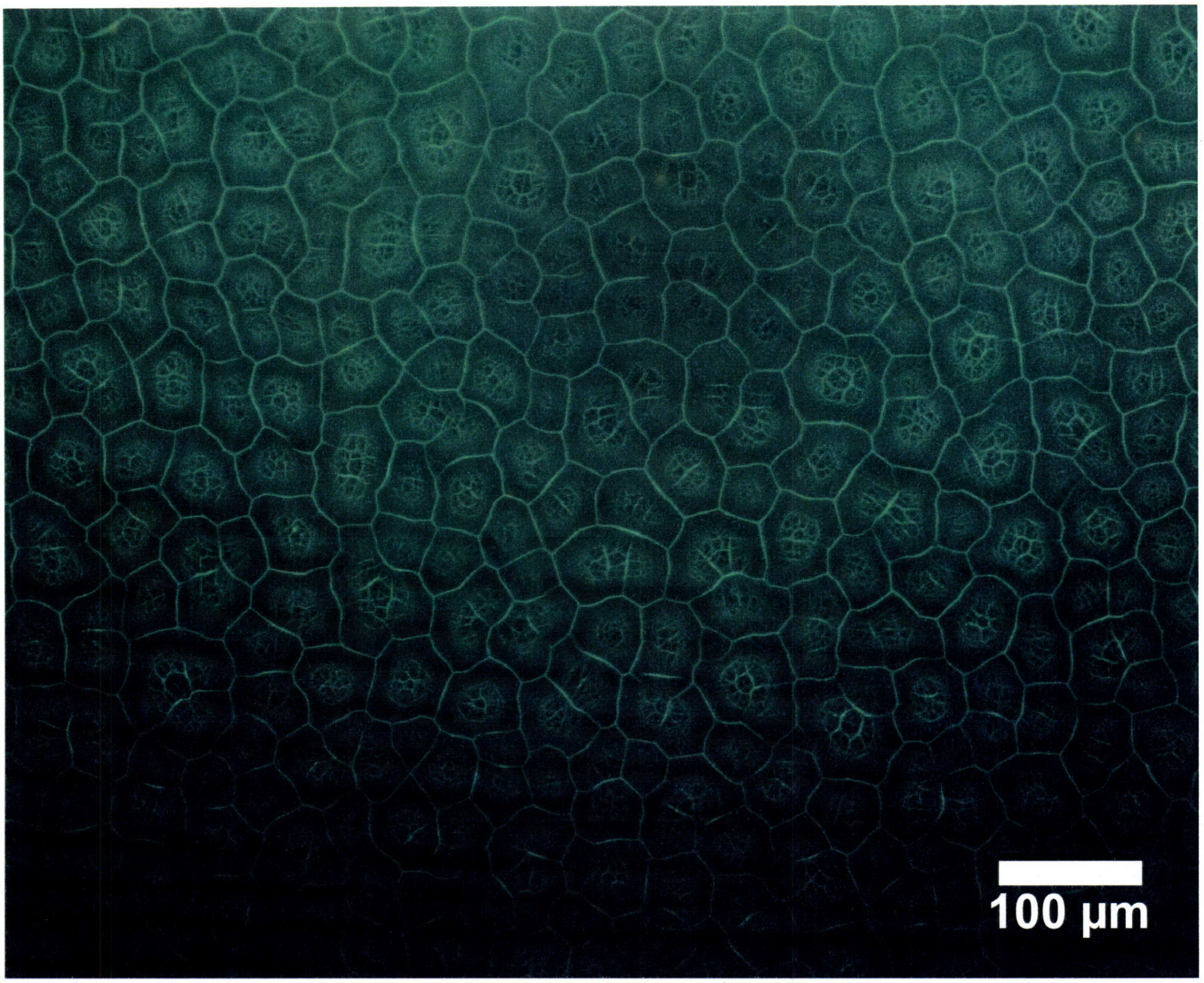

Figure 7. Fluorescence microscopy image of 100.5 bilayer film treated with pH 8.6 PAH.

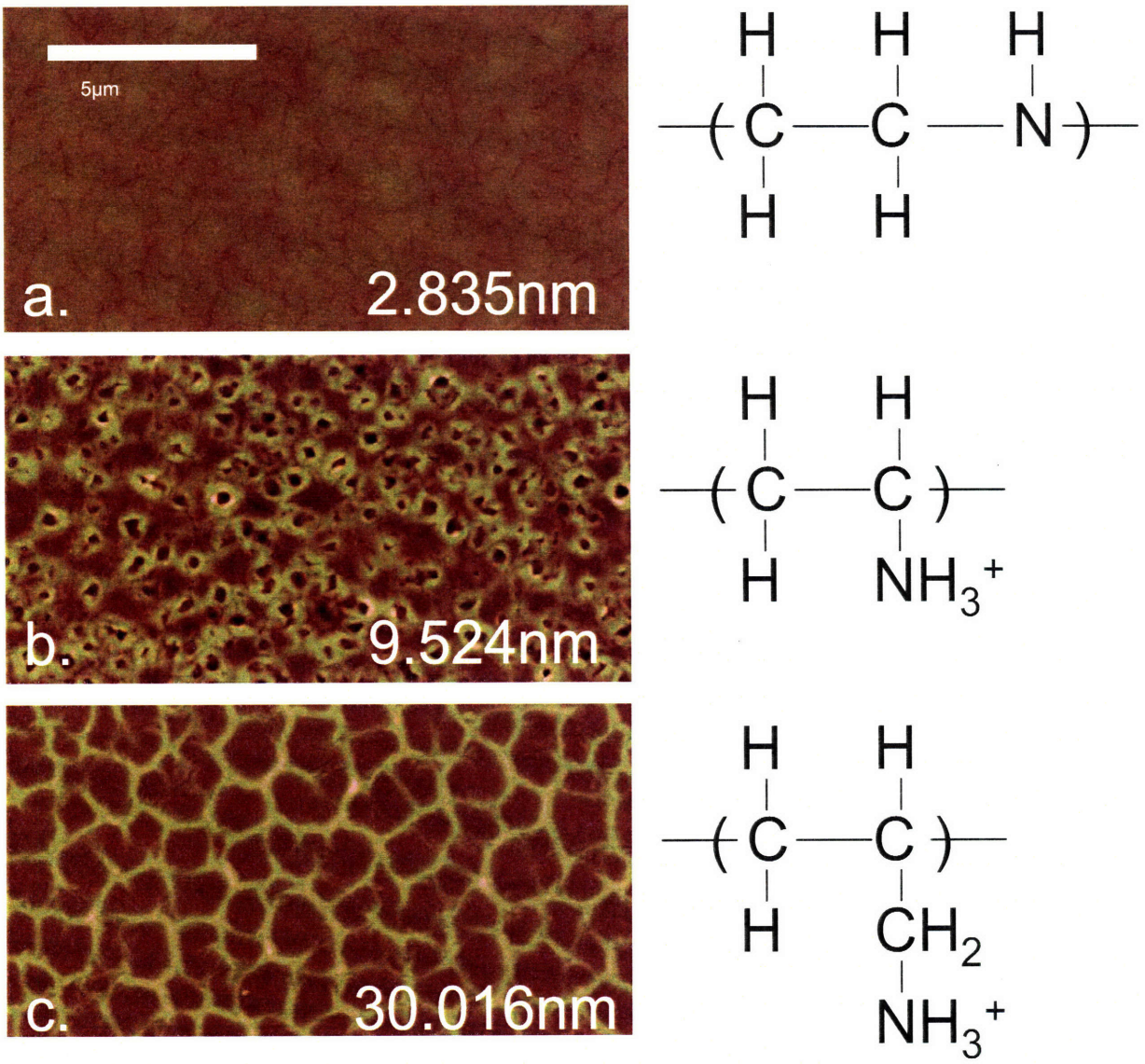

Figure 8. Increasingly hydrophobic side chains, from a) PEI (linear), b) PVAm, to c) PAH, with all treatment solutions at pH 8.6.